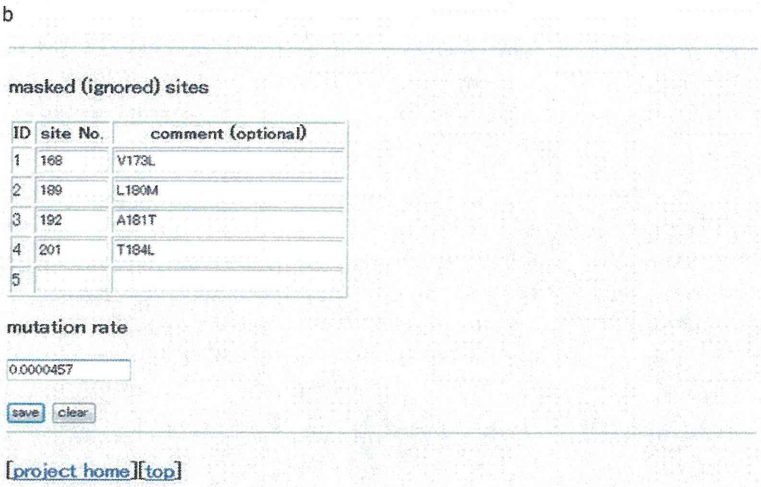

Figure 1 *Continued.*

RESULTS

Preparation of reference data

A DATASET OF all HBV S gene sequences that contain sequence variations in Japanese patients was retrieved from the HVDB[21] for reference sequences to classify suspicious samples of intrafamilial transmission. A representative sequence was selected among the same sequences in a cluster to optimize phylogenetic analysis. Full annotations of all sequences were also extracted from HVDB. The data of major genotypes were registered into the system. The results of the dataset were shown in Table 2.

Calculation for the classification of new sequences

New sequences input in query columns were calculated and then classified by the following process (Fig. 1a). The query sequences were added to the reference database described above, and the overall sequences were multiple-aligned by CLUSTAL W[22]. More precise alignment than direct alignment among queries was obtained regardless of the sequence quality of queries. Then, the genetic distance matrix was calculated from the alignment with the six-parameter method,[23] using only the sites shared by all the sequences. Finally the phylogenetic tree was constructed from the matrix using the neighbor-joining method,[24] which showed the relation among the queries, between query and published entries. The above calculation was conducted without using nucleotide positions of drug-induced resistant mutations to avoid selective pressure of antiviral treatment (Fig. 1b). As shown in Figure 1b, the mutation site of Lamivudin, Adefovir diproxil, and Entecavir resistance were masked in the present study along with the previous study.[25,26] We have estimated the substitution rate for HBV to be 4.57×10^{-5} per site per year.[27] In addition, the adjustment of age factor was calculated in consideration of genetic distance between queries for precise phylogenetic analysis (Fig. 1a). The distribution of nucleotide differences could be generally approximated by Poisson distribution and its average difference site number in the PCR amplicon of this study was 4.67 bases. The probability that two independent samples had the same sequence by chance was estimated to be less than 1%, and then the false positive data were seldom output in the intrafamilial transmission case. This system showed a sensitivity of 100% by calculating independent data retrieved from Osiowy *et al.*[28] The paper provided sequence data of a 25-year period obtained from eight asymptomatic carriers of the HBV genotype B in 1979 and 2004. For the calculation of the specificity, random sampling was performed using HVDB data. The specificity of this system was 98.6% by sampling 72 data.

Users interface

We also developed a WWW-based user interface to conduct the analysis easily. Researchers get two types of results in one analysis after they upload two or more query sequences through WWW browsers. One is a report of nucleotide difference number between

queries. This shows an indication of whether queries are similar enough or not. The other is a phylogenetic tree that shows the relation among queries and reference data.

Determination of transmission route in family cases

Four independent samples of chronic hepatitis B obtained from our hospital were tested before the analysis of suspicious intrafamilial transmission cases. Each of these four sequences was classified into distinct cluster (data not shown). As the E-PAS worked well, the analysis of suspicious intrafamilial transmission cases was examined to reveal whether two (or more) sequences obtained from a family were from intrafamilial transmission or not. The analysis was carried out by the process described above. The queries in the multiple alignments were compared between queries to count different nucleotide sites. Then, the comparison is done using the high-quality regions of the queries by ignoring ambiguous base ("N" base) sites. If three or more queries of a family were entered in the system, the comparison was calculated for each pair of queries. Table 1 shows characteristics of patients

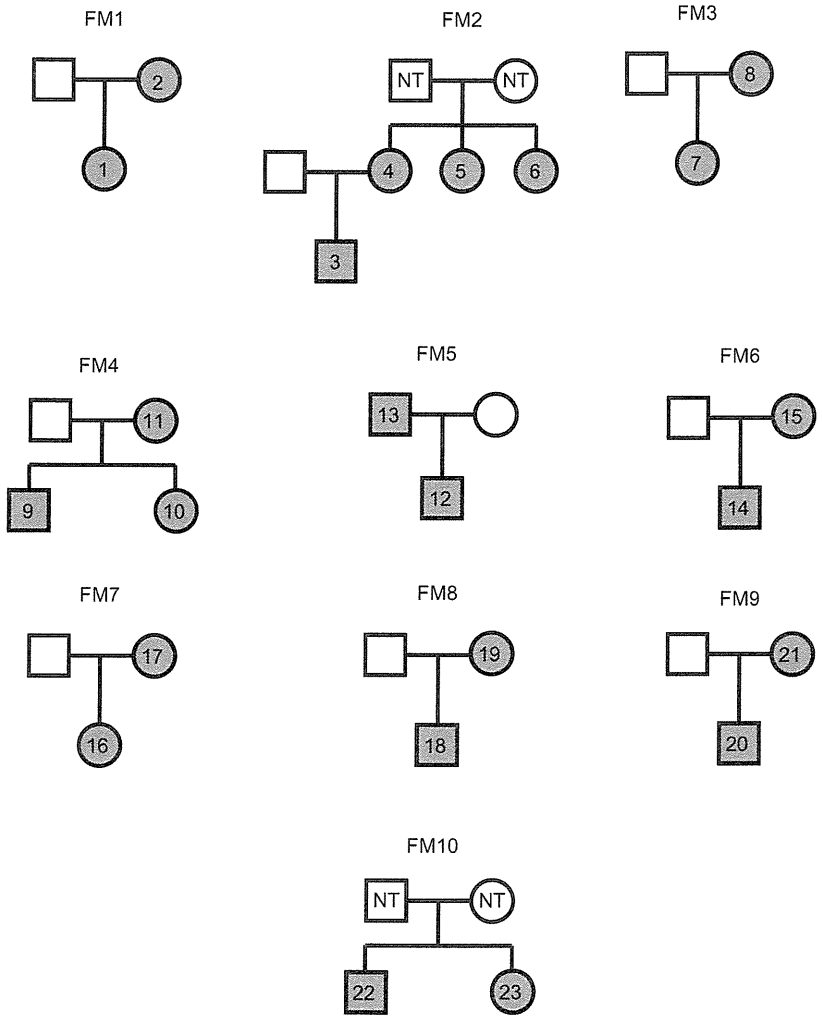

Figure 2 Family trees for 10 families with clustering hepatitis B virus (HBV) infection. Gray color indicates HBsAg positive, and white color indicates hepatitis B surface antigen (HBsAg) negative. Patients without HB antigen information are described as not tested (NT). Squares indicates male sex, circles indicates female sex.

Japanese HBV S gene classification results (user:msugiyam)

job : 20110731183753

comment : FM2

query	definition	age	nearest public entry				difference between queries									nearest cluster
			ID	subtype	overlap len	mismatch	overlap len	probe0		probe1		probe2		probe3		
								N-diff	Prob	N-diff	Prob	N-diff	Prob	N-diff	Prob	
probe0	Child	7	AB246345	C	250	2	244	0	1	0	1	0	1	4	0.000000e+00	AB246345
probe1	Mother, Sister1	41	AB246345	C	249	1		0	1	0	1	0	1	4	0.000000e+00	AB246345, probe0
probe2	Sister2	27	AB246345	C	248	0		0	1	0	1	0	1	4	0.000000e+00	AB246345, probe0, probe1
probe3	Sister3	30	AB222735	C	246	2		4	0.000000e+00	4	0.000000e+00	4	0.000000e+00	0	1	AB247916, AB222735

Figure 3 WWW-based user interface and the results of the matrix calculation by the software. The queries registered on the system were multi-aligned and analyzed for the calculation of mismatched nucleotides between the members of the family. This figure shows a representative result using FM2 data. The definition column presents sample information. The age column shows the point when their sera was collected. The nearest public entry shows the data locating near the query and displays the genotype, the length of query, and mismatched nucleotides compared with the nearest reference entry. The column of the difference between queries represents the mismatched nucleotides between the queries. The N-diff column shows the mismatched nucleotides between the queries. The probability value of the difference between two queries displays the prob column.

infected with HBV. These 10 families were analyzed to determine the transmission route using the present system. Predictably, two or three sequence data obtained from one family were classified into one cluster except for FM2 case (data not shown), and then the transmission routes of these nine families were intrafamilial as was expected.

A case of multiple transmission routes in a family

Interestingly, the result of FM2 case was different from the others. As shown in Table 1 and Figure 2, the family consisted of four carriers (three sisters and one of their sons). The number of nucleotide differences was calculated after the multiple-alignment by CLUSTAL W. Sample ID 6 (sister 3, S3) showed four mismatched nucleotides compared with the other members in the family (see the column of difference between queries in Fig. 3), and then the phylogenetic tree was described using E-PAS in HVDB. As shown in Figure 4, the sequence of ID 6 was classified into the cluster far from the other member, suggesting that ID 6 was infected with a different HBV clone from the other member. The probability value (abbreviated as Prob in Fig. 3) of intrafamilial transmission between two queries is displayed in the browser.

DISCUSSION

WE HAVE DEVELOPED an easy-to-use system for the calculation of phylogenetic analysis. The present system (E-PAS) was constructed for non-specialist users of genetics as well as specialists and would provide the appropriate results with several adjusted parameters by just preparing sequence data. Therefore, this system is recommended to users who want to easily investigate transmission routes of samples. In the present study, we have applied the E-PAS to the determination of transmission routes in families. Almost all of the family-cases showed intrafamilial transmission because the queries belonging to one family were classified in same cluster or a neighboring position. In the analysis between families, these queries certainly were located in the distinct cluster. One patient (sample ID 6) showed quite different sequences from the other members of her family. We did not determine whether her transmission route was vertical or horizontal as data of her parents on HBV infection were not provided. If both parents were HBV carriers, the different sequences could be detectable among ID 4, 5, and 6 as an intrafamilial transmission from father or mother to child, or she was infected by a vertical transmission from non-familial member.

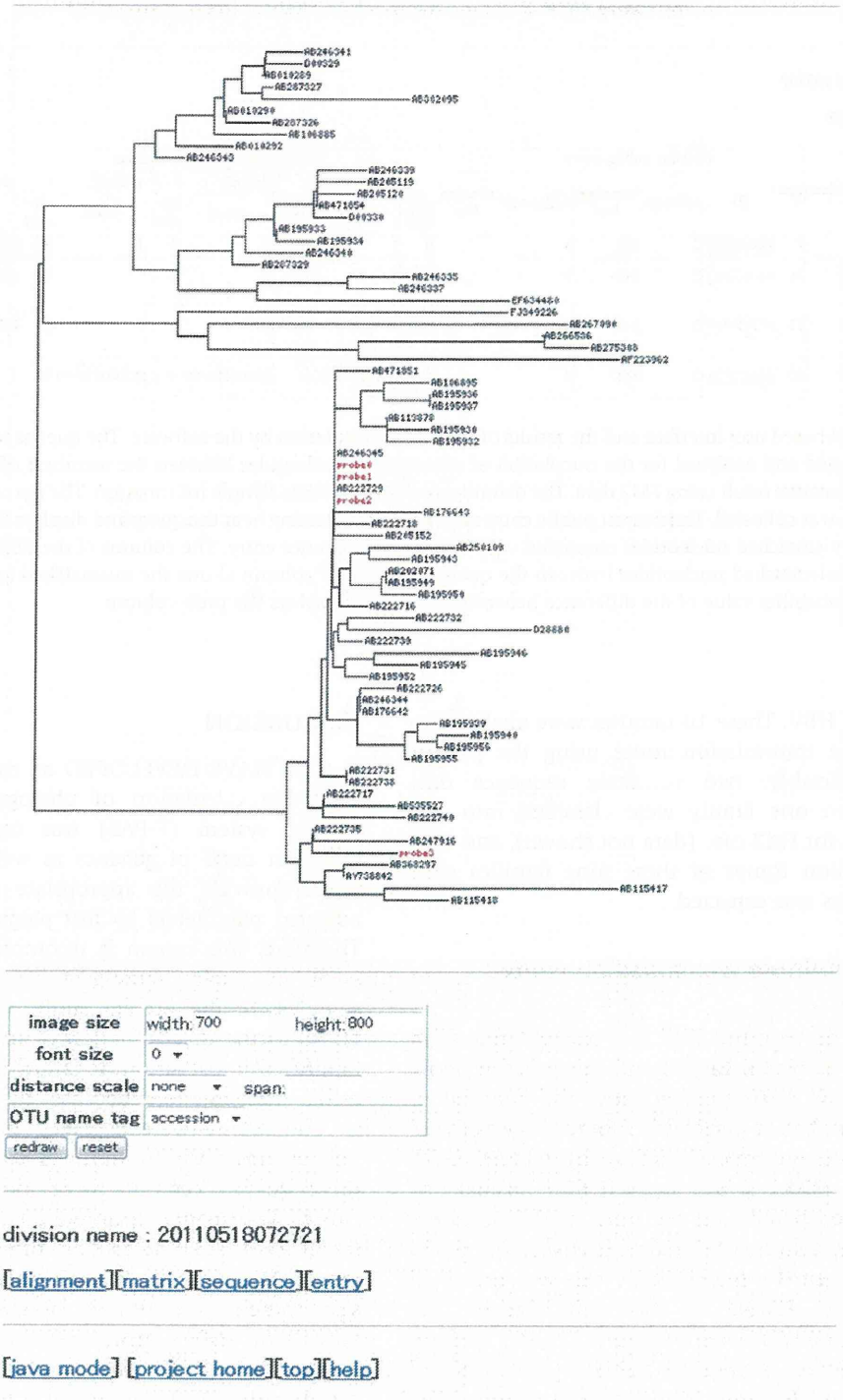

Figure 4 WWW-based user interface and the results of the phylogenetic tree. The phylogenetic tree was calculated based on the matrix data of mismatched nucleotides. A representative result using FM2 data was shown. The character in red indicates the queries. Three members of FM2 had the same sequence in the S region and were classified into the same cluster, whereas sample ID 6 (showed as probe 3 in tree) was classified into another cluster.

The primer set designed in the S region revealed high sensitive amplification because samples with low titer of HBV DNA under the limit of measurement were amplified effectively and the single band was detected in almost all samples by only the 1st PCR. Although we have estimated the substitution rate for HBV to be 4.57×10^{-5} per site per year,[27] the amplified region is a relatively highly conserved area even under antiviral drug pressure[29,30] and the region shows the genotype-dependent sequence. Therefore, a transmission route of sample ID 6 could be divided from that of the other family members. In line with this result, the determination of transmission routes and/or genotyping was achieved sufficiently even if HBV DNA was negative in conventional diagnosis. Therefore, these procedures should be determined with great caution to avoid contamination by trained researchers. The software based on a WWW-browser was customized to fit a Japanese population for quick calculation by reducing entry sequences of foreign origin. Additional datasets are under development because the present system focused on genotype B and C that are originally prevalent in Japan.

This is a versatile tool as the route of suspicious intrafamilial transmission and the genotype were determined in this assay. HBV/A has recently spread out among the young heterosexual population in addition to men who have sex with men.[16,18,19] The determination of transmission routes could contribute to epidemiological research and/or the decision of government policy to prevent the spread of HBV/A. Generally, acute hepatitis B in adulthood becomes chronic in only <1% of cases, which is much less frequent than that in Europe and the United States (approximately 10%). Since HBV/A has been more frequently observed recently in Japan, especially in metropolitan areas, HBV/A infection could provide an increased risk of chronic diseases. Further, HBV/A might be a majority of HBV infection in Japan. Reference sequence of HBV/A registered on this system could be also the appropriate reference for genotyping of HBV/A extracted from Japanese because the HBV/A2 isolates detected in Japan were homologous to those from Europe and the United States in the phylogenetic analysis.[19]

In conclusion, we have developed the easy-to-use system, E-PAS, to determine the transmission route. E-PAS separated one case infected with a clone that was different from the family, which had been expected to be intrafamilial transmission. The system is expected to accelerate the phylogenetic analysis for researchers or physicians who are not familiar with molecular genetics. Although the E-PAS has been primarily developed for Japanese patients, we are planning to extend the application for other patients by collecting foreign samples and reference sequences in addition to improve the calculation method of genetic distance.

ACKNOWLEDGMENTS

THIS WORK WAS supported by a Grant-in-Aid from the Ministry of Health Labor and Welfare of Japan and a Grant-in-Aid for JSPS Fellows of the Ministry of Education, Culture, Sports, Science, and Technology of Japan. The authors thank Professor Takashi Gojobori, National Institute of Genetics and Professor Yoshiyuki Suzuki, Nagoya City University for their professional opinion and technical support. We also thank Ms. Masako Awano, Ms. Miwa Noda, Ms. Ryuko Izumida, Ms. Mikako Kajio, and Ms. Mika Saito for their secretarial support. Laboratory work performed by Ms. Sachiko Sato, Ms. Miki Yoshida, Ms. Chieko Haga, Ms. Mami Ohashi, and Ms. Naomi Nomura is highly appreciated.

REFERENCES

1 Arauz-Ruiz P, Norder H, Robertson BH, Magnius LO. Genotype H: a new Amerindian genotype of hepatitis B virus revealed in Central America. *J Gen Virol* 2002; **83**: 2059–73.
2 Chang MH. Impact of hepatitis B vaccination on hepatitis B disease and nucleic acid testing in high-prevalence populations. *J Clin Virol* 2006; **36** (Suppl 1): S45–50.
3 Chen DS. Hepatitis B vaccination: the key towards elimination and eradication of hepatitis B. *J Hepatol* 2009; **50**: 805–16.
4 Kao JH, Chen DS. Global control of hepatitis B virus infection. *Lancet Infect Dis* 2002; **2**: 395–403.
5 Tada H, Uga N, Fuse Y *et al.* Prevention of perinatal transmission of hepatitis B virus carrier state. *Acta Paediatr Jpn* 1992; **34**: 656–9.
6 Stevens CE, Beasley RP, Tsui J, Lee WC. Vertical transmission of hepatitis B antigen in Taiwan. *N Engl J Med* 1975; **292**: 771–4.
7 Sung JL, Chen DS. Maternal transmission of hepatitis B surface antigen in patients with hepatocellular carcinoma in Taiwan. *Scand J Gastroenterol* 1980; **15**: 321–4.
8 Szmuness W, Prince AM, Hirsch RL, Brotman B. Familial clustering of hepatitis B infection. *N Engl J Med* 1973; **289**: 1162–6.
9 Lok AS, Lai CL, Wu PC, Wong VC, Yeoh EK, Lin HJ. Hepatitis B virus infection in Chinese families in Hong Kong. *Am J Epidemiol* 1987; **126**: 492–9.

10 Dumpis U, Holmes EC, Mendy M *et al.* Transmission of hepatitis B virus infection in Gambian families revealed by phylogenetic analysis. *J Hepatol* 2001; **35**: 99–104.
11 Okamoto H, Tsuda F, Sakugawa H *et al.* Typing hepatitis B virus by homology in nucleotide sequence: comparison of surface antigen subtypes. *J Gen Virol* 1988; **69** (Pt 10): 2575–83.
12 Norder H, Courouce AM, Magnius LO. Complete genomes, phylogenetic relatedness, and structural proteins of six strains of the hepatitis B virus, four of which represent two new genotypes. *Virology* 1994; **198**: 489–503.
13 Stuyver L, De Gendt S, Van Geyt C *et al.* A new genotype of hepatitis B virus: complete genome and phylogenetic relatedness. *J Gen Virol* 2000; **81**: 67–74.
14 Orito E, Ichida T, Sakugawa H *et al.* Geographic distribution of hepatitis B virus (HBV) genotype in patients with chronic HBV infection in Japan. *Hepatology* 2001; **34**: 590–4.
15 Kobayashi M, Ikeda K, Arase Y *et al.* Change of hepatitis B virus genotypes in acute and chronic infections in Japan. *J Med Virol* 2008; **80**: 1880–4.
16 Yano K, Tamada Y, Yatsuhashi H *et al.* Dynamic epidemiology of acute viral hepatitis in Japan. *Intervirology* 2010; **53**: 70–5.
17 Suzuki Y, Kobayashi M, Ikeda K *et al.* Persistence of acute infection with hepatitis B virus genotype A and treatment in Japan. *J Med Virol* 2005; **76**: 33–9.
18 Yotsuyanagi H, Okuse C, Yasuda K *et al.* Distinct geographic distributions of hepatitis B virus genotypes in patients with acute infection in Japan. *J Med Virol* 2005; **77**: 39–46.
19 Matsuura K, Tanaka Y, Hige S *et al.* Distribution of hepatitis B virus genotypes among patients with chronic infection in Japan shifting toward an increase of genotype A. *J Clin Microbiol* 2009; **47**: 1476–83.
20 Mizokami M, Gojobori T, Lau JY. Molecular evolutionary virology: its application to hepatitis C virus. *Gastroenterology* 1994; **107**: 1181–2.
21 Shin IT, Tanaka Y, Tateno Y, Mizokami M. Development and public release of a comprehensive hepatitis virus database. *Hepatol Res* 2008; **38**: 234–43.
22 Thompson JD, Higgins DG, Gibson TJ. CLUSTAL W: improving the sensitivity of progressive multiple sequence alignment through sequence weighting, position-specific gap penalties and weight matrix choice. *Nucleic Acids Res* 1994; **22**: 4673–80.
23 Gojobori T, Ishii K, Nei M. Estimation of average number of nucleotide substitutions when the rate of substitution varies with nucleotide. *J Mol Evol* 1982; **18**: 414–23.
24 Saitou N, Nei M. The neighbor-joining method: a new method for reconstructing phylogenetic trees. *Mol Biol Evol* 1987; **4**: 406–25.
25 Locarnini SA, Yuen L. Molecular genesis of drug-resistant and vaccine-escape HBV mutants. *Antivir Ther* 2010; **15**: 451–61.
26 Zoulim F, Locarnini S. Hepatitis B virus resistance to nucleos(t)ide analogues. *Gastroenterology* 2009; **137**: 1593–608 e1-2.
27 Orito E, Mizokami M, Ina Y *et al.* Host-independent evolution and a genetic classification of the hepadnavirus family based on nucleotide sequences. *Proc Natl Acad Sci USA* 1989; **86**: 7059–62.
28 Osiowy C, Giles E, Tanaka Y, Mizokami M, Minuk GY. Molecular evolution of hepatitis B virus over 25 years. *J Virol* 2006; **80**: 10307–14.
29 Mizokami M, Orito E, Ohba K, Ikeo K, Lau JY, Gojobori T. Constrained evolution with respect to gene overlap of hepatitis B virus. *J Mol Evol* 1997; **44** (Suppl 1): S83–90.
30 Pallier C, Castera L, Soulier A *et al.* Dynamics of hepatitis B virus resistance to lamivudine. *J Virol* 2006; **80**: 643–53.

Hepatology Research

Hepatology Research 2012 doi: 10.1111/j.1872-034X.2012.01013.x

Original Article

Factors responsible for the discrepancy between *IL28B* polymorphism prediction and the viral response to peginterferon plus ribavirin therapy in Japanese chronic hepatitis C patients

Hiroaki Saito,[1,2] Kiyoaki Ito,[1] Masaya Sugiyama,[1] Teppei Matsui,[1] Yoshihiko Aoki,[1] Masatoshi Imamura,[1] Kazumoto Murata,[1] Naohiko Masaki,[1] Hideyuki Nomura,[3] Hiroshi Adachi,[4] Shuhei Hige,[5] Nobuyuki Enomoto,[6] Naoya Sakamoto,[7] Masayuki Kurosaki,[8] Masashi Mizokami[1] and Sumio Watanabe[2]

[1]*The Research Center for Hepatitis and Immunology, National Center for Global Health and Medicine, Ichikawa,* [2]*Department of Gastroenterology, Juntendo University School of Medicine, Bunkyoku,* [3]*The Center for Liver Diseases, Shin-Kokura Hospital, Kitakyushu, Fukuoka,* [4]*Department of Virology and Liver Unit, Tonami General Hospital, Tonami,* [5]*Department of Internal Medicine, Hokkaido University Graduate School of Medicine, Sapporo,* [6]*Department of Internal Medicine, University of Yamanashi, Kofu,* [7]*Department for Hepatitis Control, Tokyo Medical and Dental University, Tokyo, and* [8]*Division of Gastroenterology and Hepatology, Musashino Red Cross Hospital, Musashino, Japan*

Aim: *IL28B* polymorphisms serve to predict response to pegylated interferon plus ribavirin therapy (PEG IFN/RBV) in Japanese patients with chronic hepatitis C (CHC) very reliably. However, the prediction by the *IL28B* polymorphism contradicted the virological response to PEG IFN/RBV in some patients. Here, we aimed to investigate the factors responsible for the discrepancy between the *IL28B* polymorphism prediction and virological responses.

Methods: CHC patients with genotype 1b and high viral load were enrolled in this study. In a case–control study, clinical and virological factors were analyzed for 130 patients with rs8099917 TT genotype and 96 patients with rs8099917 TG or GG genotype who were matched according to sex, age, hemoglobin level and platelet count.

Results: Higher low-density lipoprotein (LDL) cholesterol, lower γ-glutamyltransferase and the percentage of wild-type phenotype at amino acids 70 and 91 were significantly associated with the rs8099917 TT genotype. Multivariate analysis showed that rs8099917 TG or GG genotype, older age and lower LDL cholesterol were independently associated with the non-virological responder (NVR) phenotype. In patients with rs8099917 TT genotype (predicted as virological responder [VR]), multivariate analysis showed that older age was independently associated with NVR. In patients with rs8099917 TG or GG genotype (predicted as NVR), multivariate analysis showed that younger age was independently associated with VR.

Conclusion: Patient age gave rise to the discrepancy between the prediction by *IL28B* polymorphism and the virological responses, suggesting that patients should be treated at a younger age.

Key words: aging, genotype, IL28B, low-density lipoprotein cholesterol, single nucleotide polymorphism

INTRODUCTION

HEPATITIS C VIRUS (HCV) infection is a global health problem with worldwide estimates of 120–130 million carriers.[1] Chronic HCV infection, the leading cause of liver transplantation, can lead to progressive liver disease, resulting in cirrhosis and complications, including decompensated liver disease and hepatocellular carcinoma.[2] The current standard-of-care treatment for suitable patients with chronic HCV infection consists of pegylated interferon-α-2a or -2b (PEG IFN) given by injection in combination with oral ribavirin (RBV) for 24 or 48 weeks, depending on HCV genotype. Large-scale treatment in the USA and Europe showed that 42–52% of patients with HCV genotype 1

Correspondence: Dr Masashi Mizokami, The Research Center for Hepatitis and Immunology, National Center for Global Health and Medicine, 1-7-1 Kohnodai, Ichikawa, Chiba 272-8516, Japan. Email: mmizokami@hospk.ncgm.go.jp

Received 23 February 2012; revision 18 March 2012; accepted 22 March 2012.

achieved a sustained virological response (SVR),[3-5] and studies conducted in Japan produced similar results. This treatment is associated with well-known side-effects (e.g. influenza-like syndrome, hematological abnormalities and neuropsychiatric events) resulting in reduced compliance and fewer patients completing treatment.[6] It is important to predict an individual's response before treatment with PEG IFN/RBV to avoid side-effects, as well as to reduce the treatment cost. The HCV genotype, in particular, is used to predict the response: patients with the HCV genotype 2/3 have a relatively high rate of SVR (70–80%) with 24 weeks of treatment, whereas those infected with genotype 1 have a much lower rate of SVR, despite 48 weeks of treatment.[5]

Our recent genome-wide association studies (GWAS) revealed that several highly correlated common single nucleotide polymorphisms (SNP) in the region of the interleukin-28B (*IL28B*) gene on chromosome 19, coding for interferon (IFN)-λ3, are implicated in the non-virological responder (NVR) to PEG IFN/RBV phenotype among patients infected by HCV genotype 1.[7] The association between response to PEG IFN/RBV and SNP associated with *IL28B* was concurrently reported by two other groups who also employed GWAS.[8,9] The *IL28B* polymorphism was highly predictive of the response to PEG IFN/RBV therapy in Japanese chronic hepatitis C (CHC) patients.[10-12] However, this was not always the case. Therefore, we attempted to determine why the *IL28B* polymorphism did not predict the response of all patients. The nature of the functional link between the *IL28B* polymorphism and HCV clearance is unknown, and this must be defined to understand how the *IL28B* polymorphism correlates with HCV clearance. Therefore, we also investigated the association between the *IL28B* polymorphism and clinical characteristics of CHC patients.

METHODS

Patients

A TOTAL OF 696 CHC patients with genotype 1b and high viral load were recruited from the National Center for Global Health and Medicine, Hokkaido University Hospital, Tokyo Medical and Dental University Hospital, Yamanashi University Hospital, Tonami General Hospital, and Shin-Kokura Hospital in Japan. In a case–control study, sex, age, hemoglobin level and platelet count were matched between patients with the rs8099917 TT genotype ($n = 130$) and patients with rs8099917 TG or GG genotypes ($n = 96$) to eliminate background biases.

Each patient was treated with PEG IFN-α-2b (1.5 μg/kg s.c. weekly) or PEG IFN-α-2a (180 μg/body s.c. weekly) plus RBV (600–1000 mg daily, depending on bodyweight). Because a reduction in the dose of PEG IFN/RBV can contribute to a lower SVR rate,[13] only patients with an adherence of more than 80% dose for both drugs during the first 12 weeks were included in this study. Those positive for hepatitis B surface antigen and/or anti-HIV were excluded from this study.

Non-virological response was defined as less than a 2 log-unit decline in the serum level of HCV RNA from the pretreatment baseline value within the first 12 weeks and detectable viremia 24 weeks after treatment. Virological response (VR) was defined as attaining SVR or transient virological response (TVR) in this study; SVR was defined as undetectable HCV RNA in serum 6 months after treatment, whereas TVR was defined as a reappearance of HCV RNA in serum after the treatment was discontinued for a patient who had undetectable HCV RNA during the therapy or on completion of the therapy. At the time of enrollment, written informed consent was obtained for the collection and storage of serum and peripheral blood. This study was conducted in accordance with provisions of the Declaration of Helsinki.

Clinical and laboratory data

The sex, age, hemoglobin (Hb) and platelet counts were matched between study groups. Other parameters determined were as follows: alkaline phosphatase (ALP), alanine transaminase (ALT), total cholesterol, fasting blood sugar (FBS), low-density lipoprotein (LDL) cholesterol, γ-glutamyl transpeptidase (γ-GTP), α-fetoprotein (AFP), HCV RNA level and the rs8099917 polymorphism near *IL28B*.

DNA extraction

Genomic DNA was extracted from the buffy coat fraction of patients' whole blood using a GENOMIX kit (Talent SRL; Trieste, Italy).

IL28B genotyping

We have reported that the rs8099917 polymorphism is the best predictor for the response of Japanese CHC patients to PEG IFN/RBV therapy than other SNP near *IL28B*.[14] Therefore, the rs8099917 polymorphism was genotyped using the InvaderPlus assay (Third Wave Japan, Tokyo, Japan), which combines polymerase

chain reaction (PCR) and the invader reaction.[15,16] The InvaderPlus assay was performed using the LightCycler LC480 (Roche Applied Science, Mannheim, Germany).

Detection of amino acid substitutions in core and NS5A regions of HCV-1b

In the present study, substitutions of amino acid residues 70 (s-aa 70) and 91 (s-aa 91), and the presence of the IFN sensitivity-determining region (ISDR) were determined by direct nucleotide sequencing. HCV RNA was extracted from serum samples at the start of patients' therapy and reverse transcribed with a random primer and SuperScript III reverse transcriptase (Life Technologies, Carlsbad, CA, USA). Nucleic acids were amplified by PCR as described.[17]

Statistical analysis

Quantitative variables were expressed as the mean ± standard error (SE) unless otherwise specified. Categorical variables were compared using a χ^2-test or Fisher's exact test, as appropriate, and continuous variables were compared using the Mann–Whitney *U*-test. $P < 0.05$ was considered statistically significant. Multivariate analysis was performed using a stepwise logistic regression model. We performed statistical analyses using STATA ver. 11.0 (StataCorp, College Station, TX, USA).

RESULTS

Patient characteristics and *IL28B* genotype in a matched case–control study

TABLE 1 SHOWS PATIENT characteristics according to *IL28B* genotype. In a matched case–control study, sex, age, Hb levels and platelet counts were matched between 130 patients with rs8099917 TT genotype and 96 patients with rs8099917 TG or GG genotype. Lower γ-GTP ($P = 0.013$) and higher LDL cholesterol levels ($P < 0.001$) were significantly associated with the TT genotype of rs8099917. The percentages of wild type of s-aa 70 and s-aa 91 of patients with the rs8099917 TT genotype were significantly higher than those of patients with rs8099917 TG or GG genotype (s-aa 70: TT vs TG + GG, 68% vs 37% [$P < 0.001$]; s-aa 91: TT vs TG + GG, 68% vs 51% [$P = 0.017$]).

Factors associated with NVR in total patients

Table 2 shows the factors associated with NVR by univariate and multivariate analyses. Univariate analysis showed that older age ($P = 0.002$), lower platelet counts ($P = 0.01$), higher γ-GTP ($P = 0.013$), lower total cholesterol ($P = 0.017$), lower LDL cholesterol ($P < 0.001$) levels and higher AFP levels ($P = 0.019$) were significantly associated with NVR. The percentage of TG or GG genotype of rs8099917 of patients with NVR was

Table 1 Univariate analysis of *IL28B* TT and TG + GG genotypes

Variable	TT genotype ($n = 130$)	TG + GG genotype ($n = 96$)	*P*-value
Sex (% male)	61 (47)	46 (48)	Matched
Age (years), mean (SE)	57.2 (0.8)	57.5 (0.9)	Matched
Hemoglobin (g/dL), mean (SE)	14.3 (0.3)	13.9 (0.2)	Matched
Platelet count (/μL), mean (SE)	16.2 (0.5)	16.0 (0.5)	Matched
ALT (IU/L), mean (SE)	79.4 (5.4)	80.5 (7.8)	0.281
ALP (IU/L), mean (SE)	273.8 (11.7)	283.9 (11.8)	0.313
γ-GTP (IU/L), mean (SE)	63.4 (6.0)	76.0 (6.4)	0.013
Total cholesterol (mg/dL), mean (SE)	177.5 (3.3)	172.3 (3.2)	0.345
LDL cholesterol (mg/dL), mean (SE)	99.0 (2.6)	83.5 (2.8)	<0.001
Fasting blood sugar (mg/dL), mean (SE)	114.1 (4.1)	104.4 (1.9)	0.97
AFP (ng/dL), mean (SE)	9.8 (1.1)	11.5 (1.6)	0.190
HCV RNA (log IU), mean (SE)	6.2 (0.1)	6.1 (0.1)	0.186
s-aa 70 wild type (%)	70/103 (68)	30/81 (37)	<0.001
s-aa 91 wild type (%)	70/103 (68)	41/81 (51)	0.017
ISDR mutation 0–1 point (%)	82/100 (82)	70/81 (86)	0.42

AFP, α-fetoprotein; ALP, alkaline phosphatase; ALT, alanine aminotransferase; γ-GTP, γ-glutamyl transpeptidase; HCV, hepatitis C virus; ISDR, interferon sensitivity-determining region; LDL, low-density lipoprotein; SE, standard error.

Table 2 Univariate and multivariate analyses of patients with chronic hepatitis C treated with PEG IFN/RBV with respect to VR and NVR

Variable	Univariate analysis			Multivariate analysis	
	VR ($n = 128$)	NVR ($n = 98$)	*P*-value	OR (95% CI)	*P*-value
Sex (% male)	65 (51)	42 (43)	0.237		
Age (years), mean (SE)	55.6 (0.8)	59.6 (0.9)	0.002	1.075 (1.012–1.143)	0.02
rs8099917 (TG or GG genotype) (%)	23/128 (18)	73/98 (74)	<0.001	25.460 (7.436–87.169)	<0.001
Hemoglobin (g/dL), mean (SE)	14.4 (0.3)	13.7 (0.2)	0.053		
Platelet count (/μL), mean (SE)	16.9 (0.5)	15.0 (0.5)	0.01		
ALT (IU/L), mean (SE)	83.9 (6.4)	74.5 (6.2)	0.116		
ALP (IU/L), mean (SE)	274.1 (12.3)	282.9 (11.2)	0.169		
γ-GTP (IU/L), mean (SE)	65.9 (6.4)	72.6 (5.6)	0.013		
Total cholesterol (mg/dL), mean (SE)	180.3 (3.1)	168.4 (3.5)	0.017		
LDL cholesterol (mg/dL), mean (SE)	100.5 (2.7)	83.5 (2.8)	<0.001	0.978 (0.956–0.999)	0.046
Fasting blood sugar (mg/dL), mean (SE)	106.6 (2.9)	114.8 (4.4)	0.058		
AFP (ng/dL), mean (SE)	9.6 (1.1)	12.0 (1.6)	0.021		
HCV RNA (Log IU), mean (SE)	6.2 (0.1)	6.2 (0.1)	0.876		
s-aa 70 wild type (%)	67/102 (66)	33/82 (54)	0.001		
s-aa 91 wild type (%)	67/102 (66)	44/82 (54)	0.097		
ISDR mutation 0–1 point (%)	79/96 (82)	73/85 (86)	0.511		

AFP, α-fetoprotein; ALP, alkaline phosphatase; ALT, alanine aminotransferase; CI, confidence interval; γ-GTP, γ-glutamyl transpeptidase; HCV, hepatitis C virus; ISDR, interferon sensitivity-determining region; LDL, low-density lipoprotein; NVR, non-virological response; OR, odds ratio; PEG IFN, peginterferon; SE, standard error; RBV, ribavirin; VR, virological response.

significantly higher than that of patients with VR (VR vs NVR: 23/128 [18%] vs 73/98 [74%], $P < 0.001$). The percentage of wild-type s-aa 70 in patients with NVR was significantly lower than that in patients with VR [VR vs NVR: 67/102 [66%] vs 33/82 [54%], $P = 0.001$]. Multivariate analysis showed that older age (odds ratio [OR] = 1.075; 95% confidence interval [CI] = 1.012–1.14; $P = 0.02$), TG or GG genotype of rs8099917 (OR = 25.460; 95% CI = 7.436–87.169; $P < 0.001$) and lower LDL cholesterol levels (OR = 0.978; 95% CI = 0.956–0.999; $P = 0.046$) were independently associated with NVR.

VR to treatment depending on *IL28B* genotype

In the patients with the rs8099917 TT genotype, the rates of SVR, TVR and NVR were 62%, 19% and 19%, respectively. Therefore, 19% patients were NVR, even though rs8099917 represents the TT genotype (predicted as VR). In contrast, in the patients with rs8099917 TG or GG, the rates of SVR, TVR and NVR were 14%, 10% and 76%, respectively. Therefore, 24% patients were VR, even though rs8099917 was TG or GG genotype (predicted as NVR) (Fig. 1).

Factors associated with NVR in patients with the rs8099917 TT genotype

Table 3 shows the factors associated with NVR in patients with the rs8099917 TT genotype (predicted as VR) by univariate and multivariate analyses. Univariate analysis showed that female sex ($P = 0.003$), older age

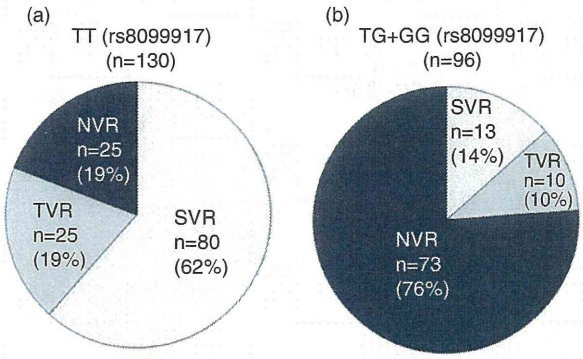

Figure 1 Virological responses to pegylated interferon and ribavirin therapy were shown in patients with rs8099917 TT (a) and TG + GG (b). NVR, non-virological response; SVR, sustained virological response; TVR, transient virological response.

Table 3 Variables associated with NVR by univariate and multivariate analyses in patients with rs8099917 TT genotype

Variable	Univariate analysis			Multivariate analysis	
	VR ($n = 105$)	NVR ($n = 25$)	*P*-value	OR (95% CI)	*P*-value
Sex (% male)	56 (53)	5 (20)	0.003		
Age (years), mean (SE)	56.1 (0.8)	61.7 (1.6)	0.001	1.142 (1.026–1.271)	0.015
Hemoglobin (g/dL), mean (SE)	14.6 (0.4)	13.1 (0.3)	0.005		
Platelet count (/μL), mean (SE)	16.7 (0.6)	13.8 (1.0)	0.019		
ALT (IU/L), mean (SE)	83.6 (6.3)	61.0 (7.9)	0.053		
ALP (IU/L), mean (SE)	270.6 (13.6)	285.9 (22.3)	0.206		
γ-GTP (IU/L), mean (SE)	66.9 (7.1)	49.2 (7.4)	0.473		
Total cholesterol (mg/dL), mean (SE)	180.2 (3.6)	165.0 (7.6)	0.072		
LDL cholesterol (mg/dL), mean (SE)	101.2 (2.9)	88.5 (5.2)	0.067		
Fasting blood sugar (mg/dL), mean (SE)	108.4 (3.5)	140.0 (15.5)	0.127		
AFP (ng/dL), mean (SE)	9.4 (1.2)	12.2 (3.6)	0.245		
HCV RNA (log IU), mean (SE)	6.2 (0.1)	6.2 (0.1)	0.948		
s-aa 70 wild type (%)	57/83 (66)	13/20 (75)	0.752		
s-aa 91 wild type (%)	55/83 (66)	15/20 (75)	0.452		
ISDR mutation 0–1 point (%)	64/79 (81)	18/21 (86)	0.618		

AFP, α-fetoprotein; ALP, alkaline phosphatase; ALT, alanine aminotransferase; CI, confidence interval; γ-GTP, γ-glutamyl transpeptidase; HCV, hepatitis C virus; ISDR, interferon sensitivity-determining region; LDL, low-density lipoprotein; NVR, non-virological response; OR, odds ratio; SE, standard error; VR, virological response.

($P = 0.001$), lower Hb levels ($P = 0.005$) and lower platelet counts ($P = 0.019$) were significantly associated with NVR in patients with the rs8099917 TT genotype. Multivariate analysis showed that only older age was independently associated with NVR in patients with the rs8099917 TT genotype (predicted as VR) (OR = 1.142; 95% CI = 1.026–1.27; $P = 0.015$).

Factors associated with VR in patients with the rs8099917 TG or GG genotypes

Table 4 shows the factors associated with VR in patients with the rs8099917 TG or GG genotypes (predicted as NVR) by univariate and multivariate analyses. Younger age ($P = 0.005$), lower γ-GTP ($P = 0.009$) and higher LDL cholesterol levels ($P = 0.032$) were significantly associated with VR by univariate analysis. Multivariate analysis showed that only younger age was independently associated with VR in patients with the rs8099917 TG or GG genotype (predicted as NVR) (OR = 0.926; 95% CI = 0.867–0.990; $P = 0.023$).

Rate of VR depending on the rs8099917 genotype of each age group

We divided patients into four age groups and compared VR rates by the differences in rs8099917 genotype for each group. The rate of VR decreased gradually in the older age groups independent of genotype. In the less than 49 years age group, the rate of VR in patients with the rs8099917 TT genotype was significantly higher than that in patients with the rs8099917 TG + GG genotypes ($P = 0.0002$). Further, in the 50–59 and 60–69 years age groups, the rates of VR in patients with the rs8099917 TT genotype were significantly higher than those in patients with the rs8099917 TG + GG genotypes ($P < 0.0001$, respectively). In the group that included subjects aged older than 69 years, only 50% of patients achieved VR even in those with the rs8099917 TT genotype (predicted as VR). In contrast, 47.6% of patients achieved VR, including those with the rs8099917 TG or GG genotypes (predicted as NVR) in the less than 49 years group (Fig. 2).

DISCUSSION

SINGLE NUCLEOTIDE POLYMORPHISM array analysis employing GWAS technology conducted by our laboratory and others revealed the relationships between SNP associated with the *IL28B* locus or present within the coding sequences for IFN-λ3, or the response to PEG IFN/RBV therapy for CHC.[7–9] Subsequent studies have confirmed that the response to PEG IFN/RBV therapy correlates with the SNP associated with *IL28B*[18,19] and indicates their value for predicting the response to PEG IFN/RBV therapy. Unfortunately, these predictions do not hold for some patients. In an attempt to understand the reasons for this, in the present study,

Table 4 Variables associated with VR by univariate and multivariate analyses in patients with rs8099917 TG or GG genotypes

Variable	Univariate analysis			Multivariate analysis	
	VR ($n = 23$)	NVR ($n = 73$)	*P*-value	OR (95% CI)	*P*-value
Sex (% male)	9 (40%)	37 (51%)	0.333		
Age (years), mean (SE)	53.2 (1.7)	58.8 (1.1)	0.005	0.926 (0.867–0.990)	0.023
Hemoglobin (g/dL), mean (SE)	13.6 (0.3)	13.9 (0.2)	0.44		
Platelet count (/μL), mean (SE)	17.6 (1.1)	15.5 (0.6)	0.059		
ALT (IU/L), mean (SE)	85.5 (21.6)	78.9 (7.8)	0.767		
ALP (IU/L), mean (SE)	291.9 (28.6)	281.8 (13.0)	0.921		
γ-GTP (IU/L), mean (SE)	62.2 (15.1)	80.4 (6.9)	0.009		
Total cholesterol (mg/dL), mean (SE)	180.5 (6.2)	169.5 (3.7)	0.17		
LDL cholesterol (mg/dL), mean (SE)	97.6 (6.9)	81.9 (3.6)	0.032		
Fasting blood sugar (mg/dL), mean (SE)	98.1 (2.8)	106.3 (2.3)	0.084		
AFP (ng/dL), mean (SE)	10.3 (3.4)	11.9 (1.8)	0.123		
HCV RNA (log IU), mean (SE)	5.9 (0.1)	6.2 (0.1)	0.087		
s-aa 70 wild type (%)	10/19 (53)	20/62 (32)	0.108		
s-aa 91 wild type (%)	12/19 (63)	29/62 (47)	0.211		
ISDR mutation 0–1 point (%)	15/17 (88)	55/64 (86)	0.806		

AFP, α-fetoprotein; ALP, alkaline phosphatase; ALT, alanine aminotransferase; CI, confidence interval; γ-GTP, γ-glutamyl transpeptidase; HCV, hepatitis C virus; ISDR, interferon sensitivity-determining region; LDL, low-density lipoprotein; NVR, non-virological response; OR, odds ratio; SE, standard error; VR, virological response.

we recruited a new set of patients for further analysis. Here, we confirmed that *IL28B* polymorphism was the most significant predictive factor for NVR with respect to PEG IFN/RBV treatment. Moreover, 19% of patients exhibiting the rs8099917 TT genotype were NVR, although they were predicted as VR. Twenty-four percent of patients with the rs8099917 TG or GG genotypes were VR, although they were predicted as NVR. We were able to determine by multivariate analysis that age was the most likely factor responsible for the discordance

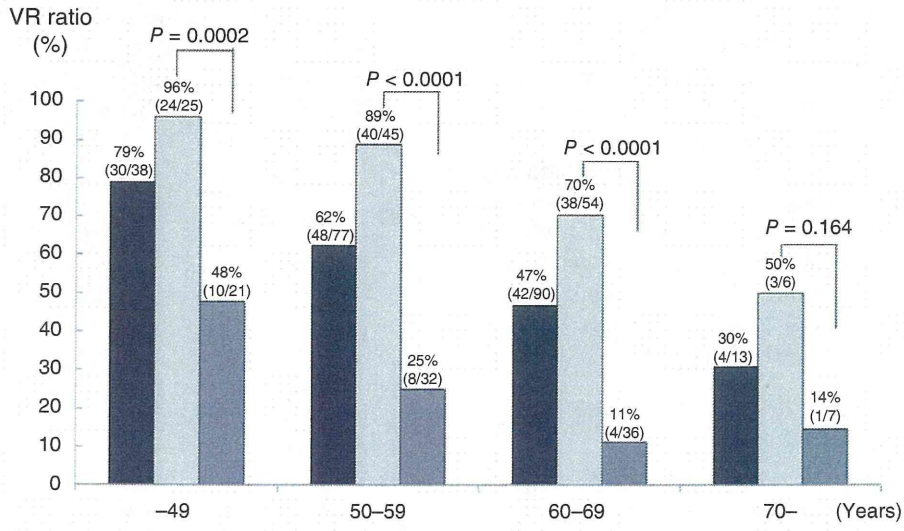

Figure 2 Virological responses (VR) to pegylated interferon and ribavirin therapy were compared between the patients with rs8099917 TT and TG + GG in each generation group. (■) Total patients, (□) TT genotype (rs8099917), (▩) TG + GG genotype (rs8099917).

between *IL28B* genotype and patients' response to viral infection.

How does age influence the VR to PEG IFN/RBV therapy? First, the lower rate of VR to PEG IFN/RBV therapy in patients with CHC was attributed to lower compliance with the IFN or RBV dose.[20,21] Because lower compliance with PEG IFN or RBV therapy was expected to be associated with a lower rate of VR in older patients, we recruited patients who were administrated over 80% of the prescribed dose of IFN/RBV. Therefore, lower compliance can be discounted as a reason for reduced response. Second, a more advanced stage of fibrosis might have been present in the older group. Platelet counts in patients with NVR were significantly lower than those in patients with VR, and lower platelet counts may be associated with advanced fibrosis.[22] Moreover, advanced fibrosis is associated with lower rates of SVR to IFN-based therapy.[23] Third, epigenetic factors such as DNA methylation induced by aging may be involved in the reduced efficacy of PEG IFN/RBV treatment in older patients. DNA methylation near gene promoters is known to turn off transcription or reduce it considerably,[24] and advanced age is strongly associated with the increased DNA methylation.[25] Therefore, DNA methylation may be increased near or in the *IL28B* promoter as a function of age resulting in suppression of *IL28B* transcription.

Lower LDL cholesterol levels were significantly associated with NVR in patients with CHC. Moreover, LDL cholesterol levels in patients with the rs8099917 TT genotype were significantly higher than those in patients with the TG + GG genotypes. The association between LDL cholesterol and *IL28B* polymorphism as well as the VR to PEG IFN/RBV has been reported.[26] Higher pretreatment levels of LDL cholesterol have been shown to predict increased response to standard PEG IFN/RBV treatment for patients with CHC.[27,28] Although the mechanisms responsible for the association between LDL cholesterol levels and the VR to PEG IFN/RBV are unknown, the *IL28B*-rs8099917 TT responder genotype, which may correlate with an increased likelihood of treatment response and higher LDL cholesterol levels, is associated with either lower IFN-λ3 activity or reduced expression of genes regulated by IFN-mediated signaling pathways.

In conclusion, our studies provide compelling evidence that patient age is most likely responsible for incorrect predictions of VR to PEG IFN/RBV therapy in Japanese CHC patients based on *IL28B* genotypes. Our findings indicated that patients should be treated as soon as they are diagnosed. It will be important to investigate the role of the epigenetic factors associated with *IL28B* expression to develop more effective PEG IFN/RBV-based therapies for patients with CHC.

ACKNOWLEDGMENT

THIS STUDY WAS supported by grants (21–112 and 21–113) from the National Center for Global Health and Medicine in Japan.

REFERENCES

1 Global Burden of Hepatitis C Working Group. Global burden of disease (GBD) for hepatitis C. *J Clin Pharmacol* 2004; **44**: 20–9.
2 Younossi Z, Kallman J, Kincaid J. The effects of HCV infection and management on health-related quality of life. *Hepatology* 2007; **45**: 806–16.
3 Fried MW, Shiffman ML, Reddy KR *et al.* Peginterferon alfa-2a plus ribavirin for chronic hepatitis C virus infection. *N Engl J Med* 2002; **347**: 975–82.
4 Manns MP, McHutchison JG, Gordon SC *et al.* Peginterferon alfa-2b plus ribavirin compared with interferon alfa-2b plus ribavirin for initial treatment of chronic hepatitis C: a randomised trial. *Lancet* 2001; **358**: 958–65.
5 Hadziyannis SJ, Sette H, Jr, Morgan TR *et al.* Peginterferon-alpha2a and ribavirin combination therapy in chronic hepatitis C: a randomized study of treatment duration and ribavirin dose. *Ann Intern Med* 2004; **140**: 346–55.
6 Bruno S, Camma C, Di Marco V *et al.* Peginterferon alfa-2b plus ribavirin for naive patients with genotype 1 chronic hepatitis C: a randomized controlled trial. *J Hepatol* 2004; **41**: 474–81.
7 Tanaka Y, Nishida N, Sugiyama M *et al.* Genome-wide association of IL28B with response to pegylated interferon-alpha and ribavirin therapy for chronic hepatitis C. *Nat Genet* 2009; **41**: 1105–9.
8 Ge D, Fellay J, Thompson AJ *et al.* Genetic variation in IL28B predicts hepatitis C treatment-induced viral clearance. *Nature* 2009; **461**: 399–401.
9 Suppiah V, Moldovan M, Ahlenstiel G *et al.* IL28B is associated with response to chronic hepatitis C interferon-alpha and ribavirin therapy. *Nat Genet* 2009; **41**: 1100–4.
10 Watanabe S, Enomoto N, Koike K *et al.* Cancer preventive effect of pegylated interferon alpha-2b plus ribavirin in a real-life clinical setting in Japan: PERFECT interim analysis. *Hepatol Res* 2011; **41**: 955–64.
11 Kurosaki M, Tanaka Y, Nishida N *et al.* Pre-treatment prediction of response to pegylated-interferon plus ribavirin for chronic hepatitis C using genetic polymorphism in IL28B and viral factors. *J Hepatol* 2011; **54**: 439–48.
12 Kurosaki M, Sakamoto N, Iwasaki M *et al.* Pretreatment prediction of response to peginterferon plus ribavirin

therapy in genotype 1 chronic hepatitis C using data mining analysis. *J Gastroenterol* 2011; **46**: 401–9.
13 McHutchison JG, Manns M, Patel K *et al.* Adherence to combination therapy enhances sustained response in genotype-1-infected patients with chronic hepatitis C. *Gastroenterology* 2002; **123**: 1061–9.
14 Ito K, Higami K, Masaki N *et al.* The rs8099917 polymorphism, when determined by a suitable genotyping method, is a better predictor for response to pegylated alpha interferon/ribavirin therapy in Japanese patients than other single nucleotide polymorphisms associated with interleukin-28B. *J Clin Microbiol* 2011; **49**: 1853–60.
15 Lyamichev V, Mast AL, Hall JG *et al.* Polymorphism identification and quantitative detection of genomic DNA by invasive cleavage of oligonucleotide probes. *Nat Biotechnol* 1999; **17**: 292–6.
16 Lyamichev VI, Kaiser MW, Lyamicheva NE *et al.* Experimental and theoretical analysis of the invasive signal amplification reaction. *Biochemistry* 2000; **39**: 9523–32.
17 Akuta N, Suzuki F, Hirakawa M *et al.* Amino acid substitution in hepatitis C virus core region and genetic variation near the interleukin 28B gene predict viral response to telaprevir with peginterferon and ribavirin. *Hepatology* 2010; **52**: 421–9.
18 Rauch A, Kutalik Z, Descombes P *et al.* Genetic variation in IL28B is associated with chronic hepatitis C and treatment failure: a genome-wide association study. *Gastroenterology* 2010; **138**: 1338–45. 45 e1–7.
19 Montes-Cano MA, Garcia-Lozano JR, Abad-Molina C *et al.* Interleukin-28B genetic variants and hepatitis virus infection by different viral genotypes. *Hepatology* 2010; **52**: 33–7.
20 Yamada G, Iino S, Okuno T *et al.* Virological response in patients with hepatitis C virus genotype 1b and a high viral load: impact of peginterferon-alpha-2a plus ribavirin dose reductions and host-related factors. *Clin Drug Investig* 2008; **28**: 9–16.
21 Bourliere M, Ouzan D, Rosenheim M *et al.* Pegylated interferon-alpha2a plus ribavirin for chronic hepatitis C in a real-life setting: the Hepatys French cohort (2003–2007). *Antivir Ther* 2012; **17**: 101–10.
22 Karasu Z, Tekin F, Ersoz G *et al.* Liver fibrosis is associated with decreased peripheral platelet count in patients with chronic hepatitis B and C. *Dig Dis Sci* 2007; **52**: 1535–9.
23 Everson GT, Hoefs JC, Seeff LB *et al.* Impact of disease severity on outcome of antiviral therapy for chronic hepatitis C: lessons from the HALT-C trial. *Hepatology* 2006; **44**: 1675–84.
24 Suzuki MM, Bird A. DNA methylation landscapes: provocative insights from epigenomics. *Nat Rev Genet* 2008; **9**: 465–76.
25 Boks MP, Derks EM, Weisenberger DJ *et al.* The relationship of DNA methylation with age, gender and genotype in twins and healthy controls. *PLoS ONE* 2009; **4**: e6767.
26 Li JH, Lao XQ, Tillmann HL *et al.* Interferon-lambda genotype and low serum low-density lipoprotein cholesterol levels in patients with chronic hepatitis C infection. *Hepatology* 2010; **51**: 1904–11.
27 Gopal K, Johnson TC, Gopal S *et al.* Correlation between beta-lipoprotein levels and outcome of hepatitis C treatment. *Hepatology* 2006; **44**: 335–40.
28 Toyoda H, Kumada T. Cholesterol and lipoprotein levels as predictors of response to interferon for hepatitis C. *Ann Intern Med* 2000; **133**: 921.

Research Article

EASL EUROPEAN ASSOCIATION FOR THE STUDY OF THE LIVER | JOURNAL OF HEPATOLOGY

Pathogenesis of lipid metabolism disorder in hepatitis C: Polyunsaturated fatty acids counteract lipid alterations induced by the core protein

Hideyuki Miyoshi[1], Kyoji Moriya[1], Takeya Tsutsumi[1], Seiko Shinzawa[1], Hajime Fujie[1], Yoshizumi Shintani[1], Hidetake Fujinaga[1], Koji Goto[1], Toru Todoroki[2], Tetsuro Suzuki[3], Tatsuo Miyamura[3], Yoshiharu Matsuura[4], Hiroshi Yotsuyanagi[1], Kazuhiko Koike[1,*]

[1]*Department of Internal Medicine, Graduate School of Medicine, University of Tokyo, Tokyo, Japan;* [2]*Department of Laboratory Medicine, Keio University School of Medicine, Tokyo, Japan;* [3]*Department of Virology II, National Institute of Infectious Diseases, Tokyo, Japan;* [4]*Department of Molecular Virology, Research Institute for Microbial Diseases, Osaka University, Osaka, Japan*

Background & Aims: Disturbance in lipid metabolism is one of the features of chronic hepatitis C, being a crucial determinant of the progression of liver fibrosis. Experimental studies have revealed that the core protein of hepatitis C virus (HCV) induces steatosis.

Methods: The activities of fatty acid metabolizing enzymes were determined by analyzing the fatty acid compositions in HepG2 cells with or without core protein expression.

Results: There was a marked accumulation of triglycerides in core-expressing HepG2 cells. While the oleic/stearic acid (18:1/18:0) and palmitoleic/palmitic acid ratio (16:1/16:0) were comparable in both the core-expressing and the control cells, there was a marked accumulation of downstream product, 5,8,11-eicosatrienoic acid (20:3(n-9)) in the core-expressing HepG2 cells. The addition of eicosatetraynoic acid, which inhibits delta-6 desaturase activity which is inherently high in HepG2 cells, led to a marked accumulation of oleic and palmitoleic acids in the core-expressing cells, showing that delta-9 desaturase was activated by the core protein. Eicosapentaenoic acid (20:5(n-3)) or arachidonic acid (20:4(n-6)) administration significantly decreased delta-9 desaturase activity, the concentration of 20:3(n-9), and triglyceride accumulation. This lipid metabolism disorder was associated with NADH accumulation due to mitochondrial dysfunction, and was reversed by the addition of pyruvate through NADH utilization.

Conclusions: The fatty acid enzyme, delta-9 desaturase, was activated by HCV core protein and polyunsaturated fatty acids counteracted this impact of the core protein on lipid metabolism. These results may open up new insights into the mechanism of lipid metabolism disorder associated with HCV infection and provide clues for the development of new therapeutic devices.

Keywords: Steatosis; Oleic acid; Core protein; Lipid metabolism; Desaturase; Hepatocellular carcinoma; NADH.

Received 31 March 2010; received in revised form 8 June 2010; accepted 5 July 2010; available online 22 September 2010

* Corresponding author. Address: Department of Gastroenterology, Graduate School of Medicine, University of Tokyo, 7-3-1 Hongo, Bunkyo-ku, Tokyo 113-8655, Japan. Tel.: +81 3 5800 8800; fax: +81 3 5800 8799.

E-mail address: kkoike-tky@umin.ac.jp (K. Koike).

Abbreviations: HCV, hepatitis C virus; HCC, hepatocellular carcinoma; PUFA, polyunsaturated fatty acids; PPAR, peroxisome proliferators-activated receptors; SREBP, sterol regulatory element binding protein; EPA, eicosapentaenoic acid; AA, arachidonic acid; ETYA, eicosatetraynoic acid; NADH, nicotinamide adenine dinucleotide; KBR, ketone body ratio.

Introduction

Persistent hepatitis C virus (HCV) infection leads to the development of chronic hepatitis, cirrhosis, and eventually, hepatocellular carcinoma (HCC), thereby being a serious problem worldwide both in medical and in socio-economical settings [1]. Histologically, several distinct features, such as bile duct damage, lymphoid follicle formation, and steatosis, (fatty change) characterize chronic hepatitis C [2–4]. Among these, steatosis is reproducible in experimental systems, both *in vitro* and *in vivo*, in which HCV proteins, particularly the core protein of HCV, are expressed. The introduced core gene induces the formation of lipid droplets in the cytoplasm of cultured cells [5,6], and in transgenic mice, it induces hepatic steatosis resembling that in chronic hepatitis C patients [7–10].

In addition, evidence has accumulated showing that steatosis is a crucial determining factor for the progression of liver fibrosis [11–13]. Steatosis and serum lipid profiles are also associated with sustained virological response to ribavirin/interferon combination therapy [14,15]. Moreover, HCV transgenic mice resemble chronic hepatitis C patients in terms of the development of HCC, implying that the HCV core protein is one of the most important viral molecules in the pathogenesis of hepatitis C [16,17]. It would thus be meaningful to explore the precise role of the core protein in modulating lipid metabolism, which may also be involved in hepatocarcinogenesis. More recently, involvement of the metabolism of lipids such as sphingolipids or cholesterol has been implicated in the replication of HCV, with a formation of lipid rafts, which are considered to be the place for HCV replication [18,19], hereby highlighting again the importance of lipid metabolism in HCV infection.

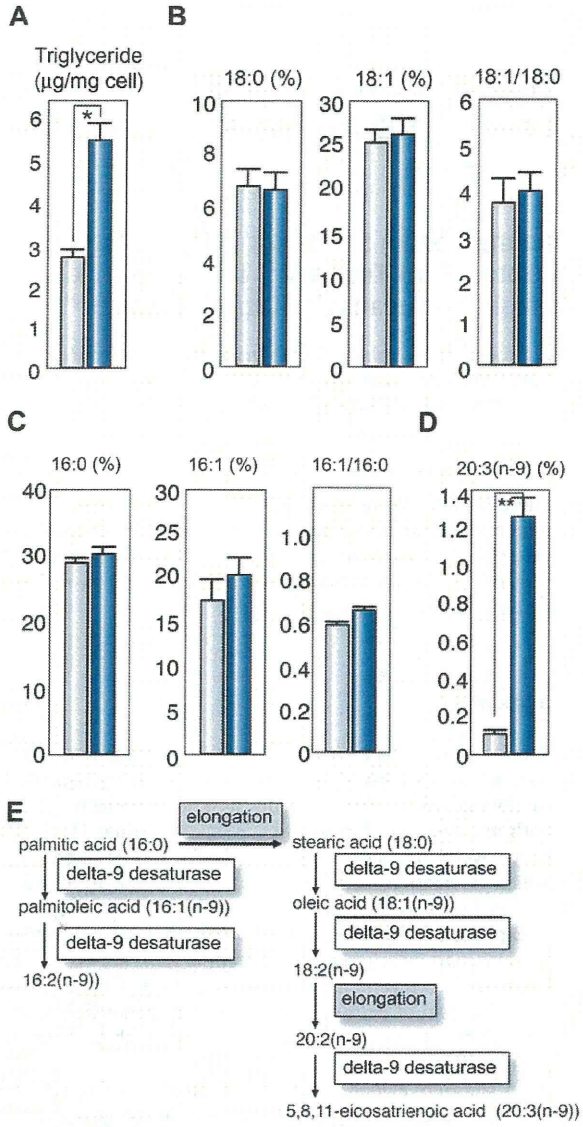

Fig. 1. Effect of the core protein on fatty acid composition in HepG2 cells. The fatty acid compositions of the total cell lipids were analyzed and the ratios of 18:1/18:0 and 16:1/16:0 in the core-expressing and control HepG2 cells were calculated. (A) Concentrations of triglycerides. (B) Percentages of stearic acid (18:0) and oleic acid (18:1(n-9)), and the 18:1/18:0 ratio. (C) Percentages of palmitic acid (16:0) and palmitoleic acid (16:1(n-9)), and the 16:1/16:0 ratio. (D) Percentage of eicosatrienoic acid (20:3(n-9). (E) Schematic display of synthetic pathway of n-9 fatty acids. Light blue bars indicate control cells and dark blue bars indicate core-expressing cells. Values represent the mean ± SE, $n = 5$ in each group. $^{*}p < 0.05$, $^{**}p < 0.01$.

Previously, we reported that the concentration of oleic acid (18:1(n-9)) was increased compared with that of stearic acid (18:0) in liver tissues of chronic hepatitis C patients as well as in those of mice transgenic for the HCV core gene [8]. Such a change may lead to increased membrane fluidity, owing to the lower melting temperature of monounsaturated fatty acids, resulting in incremental metabolism and proliferation of hepatocytes [20–22]. On the other hand, polyunsaturated fatty acids (PUFAs), such as eicosapentaenoic acid (20:5(n-3)) and arachidonic acid (20:4(n-6)), are known to activate the nuclear transcription of peroxisome proliferator-activated receptors (PPAR) and suppress the sterol regulatory element binding protein (SREBP)-1. While PPARγ induces delta-9 desaturase (stearoyl-CoA desaturase) gene expression, PUFAs suppresses delta-9 desaturase activity [23]. In the current study, we determined fatty acid desaturase activities by analyzing the fatty acid compositions in HepG2 cells expressing HCV core protein by chromatography. In addition, we determined whether exogenous PUFAs restore HCV-associated changes in fatty acid metabolism.

Materials and methods

Reagents

Eicosapentaenoic acid (EPA), arachidonic acid (AA), and eicosatetraynoic acid (ETYA) were purchased from Sigma Chemical (St. Louis, MO). Other chemicals were of analytical grade and purchased from Wako Chemicals (Tokyo, Japan).

Cell culture

This study was performed using HepG2 cell lines expressing the HCV core protein under the control of the CAG promoter (Hep39J, Hep396 and Hep397), or a control HepG2 line (Hepswx) carrying an empty vector, which were described previously [24], and control bulk HepG2 cells. They were maintained in Dulbecco's modified Eagle's medium (DMEM), supplemented with 10% fetal bovine serum (Invitrogen), 1 mg/ml G418, 100 U/ml penicillin, and 100 μg/ml streptomycin in a humidified atmosphere at 37 °C in 5% CO_2. Fatty acids were dissolved in DMEM containing defatted bovine serum albumin. The ratio of fatty acids to albumin (mole/mole) was 0.7. The cells were exposed to fatty acid–albumin complexes at various concentrations for 48 h. All the experiments were repeated at least five times.

Lipid extraction, measurement of triglyceride content, and analysis of fatty acid composition

Total cell lipids were extracted by Foch's method. The cells were washed twice with phosphate-buffered saline and collected by centrifugation. The cell pellets were homogenized with 10 vole of chloroform: methanol solution (2:1), and the mixture was shaken for 5 min. The lower phase was then washed with 4 vole of saline, dried on anhydrous sodium sulfate, and evaporated to complete dryness. For the analysis of fatty acid composition, the residue was methanolysed by the modified Morrison and Smith method with boron trifluoride as a catalyst [25]. Fatty acid methyl esters were analyzed using a Shimadzu GC-7A gas chromatograph (Shimadzu Corp., Kyoto, Japan).

Measurement of the ketone body ratio and lactate/pyruvate

The cells were cultured to confluence on 3.5 cm dishes, and the medium was replaced with 700 μl of fresh one. After 24 h of incubation, the levels of acetoacetate and β-hydroxybutyrate in the medium were measured by monitoring the production or consumption of nicotinamide adenine dinucleotide (NADH) with Ketorex kit (Sanwa Chemical, Nagoya, Japan) [26]. The ketone body ratio (KBR) was calculated as the acetoacetate/β-hydroxybutyrate ratio. The lactate and pyruvate levels in the medium were measured at random times by the lactate oxidase method and pyruvate oxidase method, respectively.

Effect of pyruvate on lipid metabolism

In some experiments, pyruvate (Wako Chemicals) was added to culture medium at a final concentration of 0, 1, 5, or 10 mM. After 48 h of incubation at 37 °C, the cells were harvested and subjected to fatty acid composition analysis or real-time PCR analysis.

Research Article

Real-time PCR

RNA was prepared from cultured cells using TRIzol LS (Invitrogen, Carlsbad, CA). The fluorescent signal was measured using ABI prism 7000 (Applied Biosystems, Tokyo, Japan). The genes encoding mouse sterol regulatory element-binding proteins (SREBP)-1a, SREBP-1c, delta-9 desaturase, and hypoxanthine phosphoribosyltransferase were amplified with the primer pairs CACAGCGGTTTTGAACGAC and CTGGCTCCTCTTTGATCCCA, ACGGAGCCATGGATTGCACATTTG and TACATCTT TAAAGCAGCGGGTGCCGATGGT, TTCCCTCCTGCAAGCTCTAC and CGCAAGAAGG TGCTAACGAAC, and CCAGCAAGCTTGCAACCTTAACCA and GTAATGATCAGTCAAC GGGGGAC, respectively.

Statistical analysis

Data are presented as the mean ± SE. The data were analyzed by Mann–Whitney *U* test. Differences were considered statistically significant when $p < 0.05$.

Results

Triglyceride content in HepG2 cells expressing HCV core protein

To validate the relationship between the lipid accumulation and the core protein, we first determined the triglyceride contents in core-protein-expressing HepG2 clones (core-expressing cells), Hep39J, Hep396, Hep397, and control HepG2 cells. Core-expressing Hep396 cells contained significantly larger amounts of triglyceride than the control cells (Fig. 1A, $p < 0.01$), which are consistent with the results of previous studies on culture cells and transgenic mice [6,7,27]. Similar results were obtained with the other core-expressing cell lines.

Fatty acid compositions of total cell lipids

Analysis on the fatty acid compositions of total lipids revealed that the concentration of oleic acid (18:1(n-9)) and the ratio of oleic acid/stearic acid (18:1/18:0) in the core-expressing cells are similar to those in the control cells (Fig. 1B). The ratio of palmitoleic acid (16:1(n-9))/palmitic acid (16:1/16:0) was higher in the core-expressing cells than that in the control cells, but the difference was not significant (Fig. 1C). This rather dissociates from the results obtained in HCV core gene transgenic mice, in which the 18:1/18:0 ratio was significantly higher than that in control mice, thereby suggesting an increased delta-9 desaturase activity as a consequence of the HCV core protein expression [8]. However, it should be noted that the concentration of 5,8,11-eicosatrienoic acid (20:3(n-9)), a downstream product of n-9 fatty acid desaturation, was approximately13 times higher in the core-expressing cells than that in the control cells (Fig. 1D and E, $p < 0.01$). This is due to the fact that the activity of the delta-6 desaturase, an enzyme downstream of delta-9 desaturase, is also high in HepG2 cells, resulting in the relatively lower concentration of 18:1 in the core-expressing cells despite the high delta-9 desaturase activity. Actually, the delta-6 desaturase activity has been shown to be inherently high in HepG2 cells [28,29].

To verify this possibility, we administered ETYA, which inhibits delta-6 desaturase activity, to the cell cultures. Because similar results were obtained with the other core-expressing HepG2 cell lines, subsequent experiments were carried out using the Hep396 cell line. The addition caused significant increases in both 18:1/18:0 and 16:1/16:0 ratios in the core-expressing cells but not in the control cells (Fig. 2A 0 vs. 10 μg/ml and 0 vs. 50 μg/ml; $p < 0.05$, respectively). When compared between the

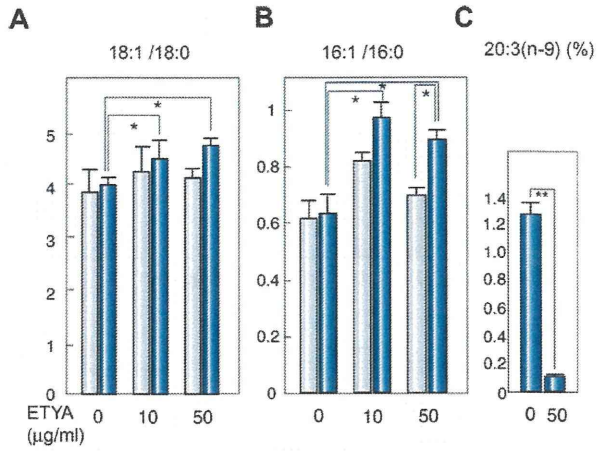

Fig. 2. Effect of ETYA on delta-9 desaturase index. HepG2 cells with or without the core protein were incubated with ETYA for 48 h. The fatty acid compositions of the total cell lipids were analyzed, and the ratios of 18:1/18:0 (A) and 16:1/16:0 (B), and the percentage of eicosatrienoic acid (20:3(n-9) (C) were computed. Light blue bars indicate control cells and dark blue bars indicate core-expressing cells. $N = 5$ in each group. *$p < 0.05$. ETYA, eicosatetraynoic acid.

core-expressing cells and control cells after the treatment with 50 μg/ml ETYA, the 18:1/18:0 ratio was higher and the 16:1/16:0 ratio was significantly higher (Fig. 2B, $p < 0.05$) in the core-expressing cells. ETYA (50 μg/ml) significantly decreased the concentration of 20:3(n-9) in the core-expressing cells (Fig. 2C, $p < 0.01$). These results suggest that the HCV core protein enhances the activities of delta-9, and possibly, delta-5 desaturases, modulating fatty acid metabolism in HepG2 cells, in which the delta-6 desaturase activity is intrinsically high (Fig. 1E) [28,29].

PUFAs modify fatty acid compositions and decrease triglyceride contents in HepG2 Cells

PUFAs are known to suppress the activities of both delta-9 and delta-6 desaturases. We, therefore, added PUFA, EPA, or AA, to the culture cell medium to examine the effect of PUFAs on the fatty acid compositions in HepG2 cells expressing the core protein. EPA and AA individually decreased the 18:1/18:0 and 16:1/16:0 ratios in a similar extent in both the core-expressing cells and the control cells (Fig. 3, $p < 0.05$). EPA and AA also significantly decreased the concentration of 20:3(n-9) in the core-expressing cells in a dose-dependent manner (Fig. 4, $p < 0.05$). In addition, EPA and AA individually decreased the triglyceride concentration in cells, in particular, in the core-expressing cells (Fig. 5, in core-expressing cells, $p < 0.01$; in control cells, $p < 0.05$, respectively).

Ketone body ratio and lactate/pyruvate ratio

Although the mechanism by which the HCV core protein enhances fatty acid desaturation is yet unclear, one possibility is the creation of an overreduced state in the core-expressing cells. The overreduced state or the accumulation of NADH in cells is known to accelerate the activities of fatty acid desaturases [30,31]. Such a condition may originate from the dysfunction of the mitochondrial electron transfer system (ETS), which has been

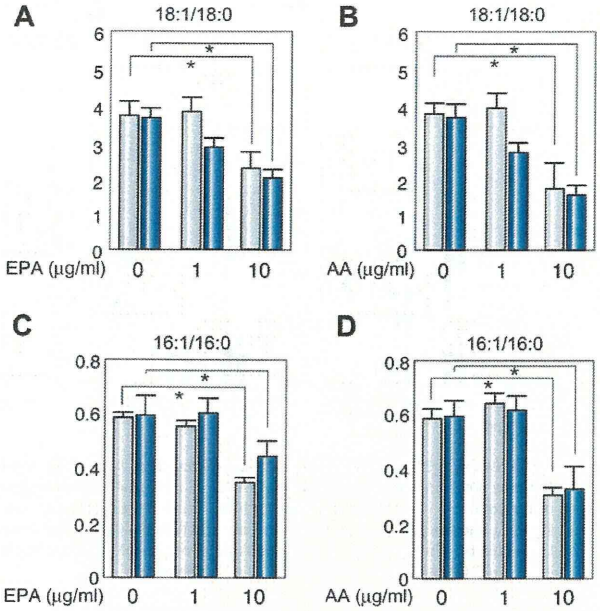

Fig. 3. Effect of EPA and AA on delta-9 desaturase index. HepG2 cells with or without the core protein were incubated with EPA (A and C) or AA (B and D) for 48 h. The fatty acid compositions of the total cell lipids were analyzed and the ratios of 18:1/18:0 (A and B) and 16:1/16:0 (C and D) were computed. Light blue bars indicate control cells and dark blue bars indicate core-expressing cells. $N = 5$ in each group. $^{*}p < 0.05$. EPA, eicosapentaenoic acid; AA, arachidonic acid.

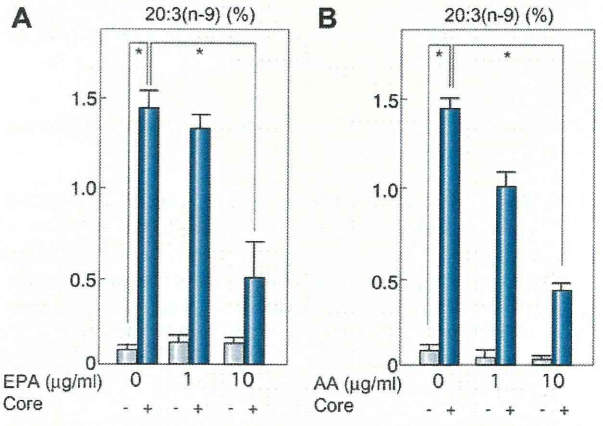

Fig. 4. Effect of EPA and AA on the concentration of 20:3(n-9). HepG2 cells with or without the core protein were incubated with EPA (A) or AA (B) for 48 h. The fatty acid compositions of the total cell lipids were analyzed and the percentages of the C20:3(n-9) fraction were measured. Light blue bars indicate control cells and dark blue bars indicate core-expressing cells. $N = 5$ in each group. $^{*}p < 0.05$.

suggested to be associated with HCV infection by the action of the HCV core protein [32–35]. Then, we explored the possibility that an increase in the NADH level, which is caused by the mitochondrial ETS dysfunction, induces the activation of fatty acid desaturases. Because fatty acid synthesis or fatty acid desaturation is accompanied by the oxidation of NAD(P)H, we measured the ketone body ratio (KBR) in the culture medium to estimate the redox state in the HepG2 cells expressing the core protein.

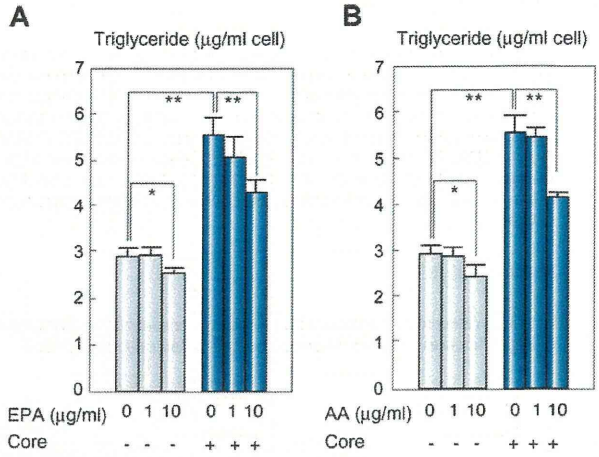

Fig. 5. Effect of EPA and AA on triglyceride content. HepG2 cells with or without the core protein were incubated with EPA (A) or AA (B) for 48 h. The triglyceride volume of the total cell lipids was measured and the triglyceride contents in the cells were calculated. Light blue bars indicate control cells and dark blue bars indicate core-expressing cells. $N = 5$ in each group. $^{*}p < 0.05$, $^{**}p < 0.01$.

The KBR, which is in equilibrium with the intramitochondrial NAD^+/NADH [26,36], in the culture medium of the core-expressing cells, was significantly lower than that of control cells (Fig. 6A, $p < 0.01$). The ratio of lactate to pyruvate (lactate/pyruvate), which is proportional to the cytosolic NADH/NAD^+ [26], in the culture medium of the core-expressing cells was significantly higher than that of control cells (Fig. 6B, $p < 0.05$). These results, the higher NADH/NAD^+ ratio in both determinations, indicate that NADH accumulates in the core-expressing HepG2 cells, resulting in the overreduced state, as a consequence of the core protein expression. The amounts of total ketone bodies were significantly higher in the core-expressing cells than that in the control cells (Fig. 6C).

Effects of pyruvate on lipid metabolism in core-expressing cells

The addition of pyruvate into this constitutive core protein expression system, in which the pyruvate metabolism is in equilibrium, is expected to cause a reduction in the NADH level along with increases in the levels of lactate and NAD^+, because pyruvate tends to be converted to lactate by the action of lactate dehydrogenase (LDH) under the condition of high NADH/NAD^+ ratio [26,36]. Actually, the addition of pyruvate into the culture medium at various concentrations increased the KBR and reduced the amount of 5,8,11-eicosatrienoic acid (20:3 (n-9)) (Fig. 6D, $p < 0.05$ at 10 mM pyruvate), while it had no effect on the control cells. It also caused a reduction in the amount of triglyceride in the core-expressing cells but not in the control cells (Fig. 6E). This finding strongly supports the notion that NADH accumulation is, at least, one of the causes of the activation of fatty acid desaturases in this HCV model. The mRNA levels of anti-oxidant genes significantly decreased after the incubation with pyruvate at 10 mM (catalase, 1.27 ± 0.06 vs. 0.91 ± 0.05; glutathione synthetase 1.39 ± 0.04 vs. 1.01 ± 0.06; glutathione peroxidase 1.48 ± 0.03 vs. 1.23 ± 0.07, pyruvate (−) vs. pyruvate (+), $p < 0.05$, respectively), suggesting that pyruvate reduced the levels of oxidative stress in the core-expressing HepG2 cells.

Research Article

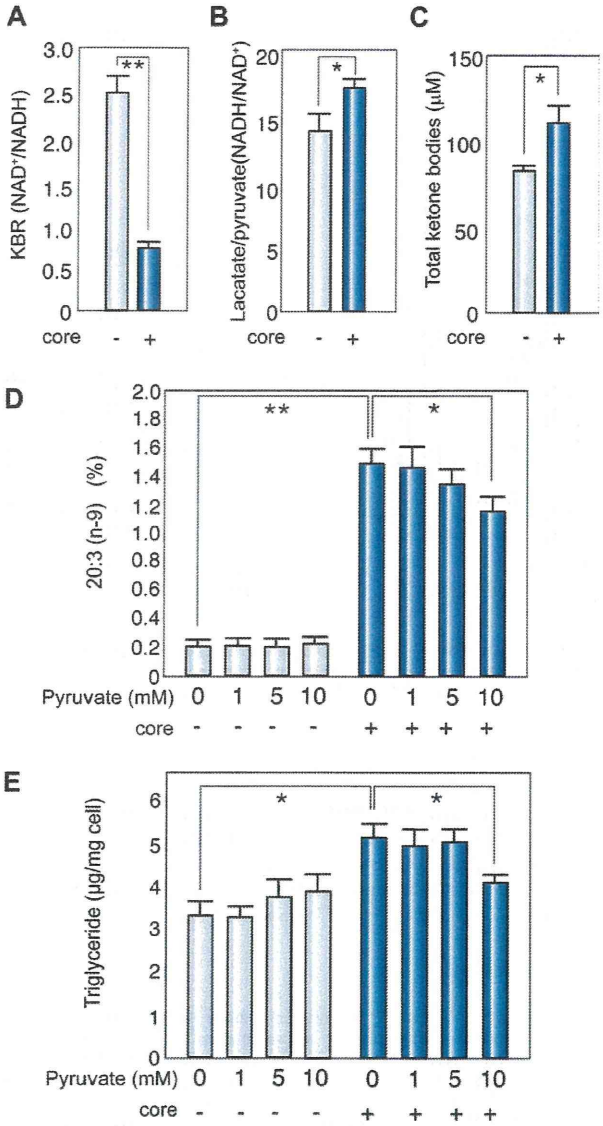

Fig. 6. NADH accumulation and effect of pyruvate in core-expressing cells. HepG2 cells with or without the core protein were subjected to the determination of ketone body ratio (A) and lactate/pyruvate ratio (B) for the precise estimation of NAD^+/NADH and NADH/NAD^+. (C) Total ketone bodies. (D) The percentages of the C20:3(n-9) fraction were measured after incubation with pyruvate at various concentrations. (E) The total amount of triglyceride was measured after incubation with pyruvate at various concentrations. Light blue bars indicate control cells and dark blue bars indicate core-expressing cells. $N = 5$ in each group. $^*p < 0.05$, $^{**}p < 0.01$.

Expression of SREBP-1 and desaturase genes in core-expressing cells

We previously showed that the core protein activates the expression of the SREBP-1c gene, which regulates the production of triglyceride [37] in the liver. We, therefore, examined the mRNA levels of genes associated with lipid metabolism in the current system. As shown in Fig. 7, the mRNA levels of SREBP-1c and delta-9 (stearoyl CoA) desaturase genes, but not that of the SREBP-1a gene, were significantly higher in the core-expressing cells than that in the control cells. Of note, the mRNA levels of the former two genes significantly decreased after the incubation with AA. The treatment with pyruvate also reduced the mRNA levels of the two genes, but the difference was not statistically significant compared with the control.

Discussion

The core protein of HCV modulated the activities of delta desaturases and changed the saturation states of fatty acids. The observed change in the HepG2 cells, namely, an increase in the amounts of unsaturated fatty acids, may support cell proliferation, by increasing the fluidity of the cell membrane as reported previously [20]. In the HepG2 cells expressing the core protein, the delta-6 desaturase activity was as high as that of the delta-9 desaturase, leading to the accumulation of a downstream product, 20:3(n-9) fatty acid. This was, unexpectedly, in contrast to our previous result on the liver tissues of HCV core gene transgenic mice, in which the 18:1/18:0 and 16:1/16:0 ratios were significantly higher than that in the liver tissues of normal littermate mice, indicating the activation of delta-9 desaturase [8]. The 16:1/16:0 and 18:1/18:0 ratios observed in the control HepG2 cells were consistent with the results of a previous study: the delta-6 desaturase activity is inherently higher in HepG2 cells than in normal mouse hepatocytes [28,29]. This may explain the difference in the effect of the core protein on lipid metabolism in these two systems, namely, HepG2 cells and mouse liver tissues. The significant increase in the delta-9 desaturase index and high concentration of 20:3(n-9) by the administration of ETYA, a delta-6 desaturase inhibitor, indicate the activation of delta-9 desaturase in the core-expressing cells. The results of real-time PCR analysis for determining the mRNA levels of these enzymes corroborated the current estimation of desaturase activities as determined by fatty acid analysis.

The mechanism underlying the activation of fatty acid desaturation by the HCV core protein is still unclear, but one possibility is the presence of an overreduced state in the core-expressing cells. The HCV core protein is closely associated with mitochondrial dysfunction, in particular, that of the respiratory chain complexes, resulting in an impairment of NADH oxidation [32–35]. NADH accumulation leads to an increase in desaturase activities through the augmentation of microsomal electron transfer [38]. In fact, the KBR in the core-expressing cells was significantly lower than that in the control cells, indicating the accumulation of NADH within the cells. The addition of pyruvate resulted in an increase in the KBR and a reduction in the amounts of triglyceride and 5,8,11-eicosatrienoic acid (20:3 (n-9)) while it had no effect on the control cells, strongly supporting the notion that NADH accumulation induced by the core protein is, at least, one of the causes of the activation of fatty acid desaturases in this HCV model.

Another possible mechanism underlying the accelerated desaturation is the activation of SREBP-1c, which controls the expression of delta-9 desaturase. In fact, the level of SREBP-1c mRNA was higher in the core-expressing cells than that in the control cells as reported previously [37]. The relief of NADH accumulation by pyruvate administration resulted in the reduced accumulation of triglyceride and unsaturated fatty acids, which was accompanied by the reduction in SREBP-1c and delta-9 desaturase gene expression levels. The intracellular accumulation of NADH might be involved in the activation of the SREBP-1c gene expression by the core protein. Thus, NADH accumulation, which

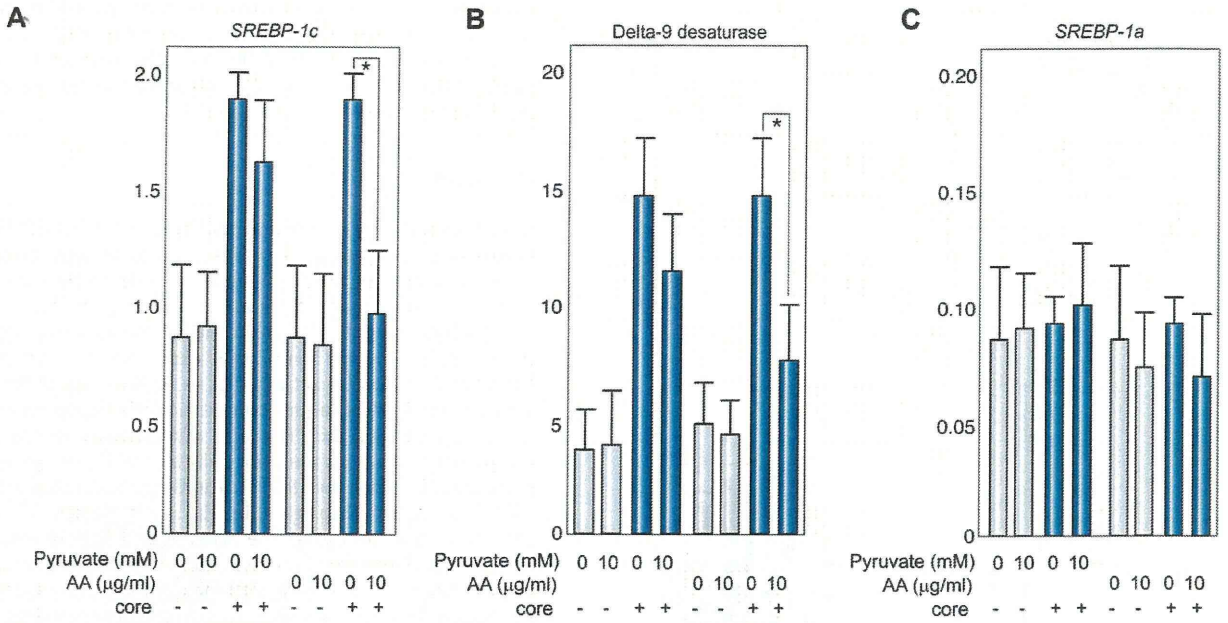

Fig. 7. Effect of pyruvate and AA on mRNA levels of lipid-associated genes. The mRNA levels of *SREBP-1c* (A), delta-9 desaturase (B) and *SREBP-1a* (C) genes were determined by real-time PCR analysis. The transcription of the genes was normalized with that of hypoxanthine phosphoribosyltransferase, and the values are expressed as relative activities. Light blue bars indicate control cells and dark blue bars indicate core-expressing cells. $N = 5$ in each group. $^*p < 0.05$. SREBP, sterol regulatory element binding protein.

is induced by the core protein through the impairment of the mitochondrial complex function [35], may be a key event that leads to the SREBP-1c activation, the desaturase activation, and the development of steatosis associated with HCV infection.

EPA and AA (PUFAs), which are known to suppress desaturase activities, lowered the 18:1/18:0 and 16:1/16:0 ratios and decreased the concentration of 20:3(n-9) concomitantly with that of triglyceride, regardless of the presence of the core protein, probably through SREBP-1c suppression (Fig. 7) [39]. On the other hand, the administration of EPA or AA did not affect the KBR in the core-expressing or control cells (data not shown), limiting the PUFAs ability to counteract the effect of the core protein. This is in contrast to the fact that the addition of pyruvate caused an increase in the KBR and a reduction in the amounts of triglyceride and 5,8,11-eicosatrienoic acid (20:3 (n-9)), while it had no effect on the control cells.

Fatty acid desaturation is closely associated with increased membrane fluidity [20], leading to augmented cell metabolism and higher cell division rates [21,22]. Although the relationship between carcinogenesis and lipid metabolism altered by the HCV core protein remains to be further clarified, alterations in lipid metabolism, in particular, in the desaturation of fatty acids, are closely associated with HCV infection, and PUFAs could prevent the pathogenesis of HCV-associated disorders involving lipid metabolism.

Conflict of interest

The authors who have taken part in this study declared that they do not have anything to disclose regarding funding or conflict of interest with respect to this manuscript.

Acknowledgments

This work was supported in part by Grant-in-Aid for Scientific Research on Priority Area from the Ministry of Education, Science, Sports, and Culture of Japan; Health Sciences Research Grants of The Ministry of Health, Labour, and Welfare (Research on Hepatitis); and a grant from The Sankyo Foundation of Life Science.

References

[1] Saito I, Miyamura T, Ohbayashi A, Harada H, Katayama T, Kikuchi S, et al. Hepatitis C virus infection is associated with the development of hepatocellular carcinoma. Proc Natl Acad Sci USA 1990;87:6547–6549.
[2] Schemer PJ, Ashrafzadeh P, Sherlock S, Brown D, Dusheiko GM. The pathology of chronic hepatitis C. Hepatology 1992;15:567–571.
[3] Bach N, Thung SN, Schaffner F. The histological features of chronic hepatitis C and autoimmune chronic hepatitis: a comparative analysis. Hepatology 1992;15:572–577.
[4] Fujie H, Yotsuyanagi H, Moriya K, Shintani Y, Tsutsumi T, Takayama T, et al. Steatosis and intrahepatic hepatitis C virus in chronic hepatitis. J Med Virol 1999;59:141–145.
[5] Moradpour D, Englert C, Wakita T, Wands JR. Characterization of cell lines allowing tightly regulated expression of hepatitis C virus core protein. Virology 1996;222:51–63.
[6] Barba G, Harper F, Harada T, Kohara M, Goulinet S, Matsuura Y, et al. Hepatitis C virus core protein shows a cytoplasmic localization and associates to cellular lipid storage droplets. Proc Natl Acad Sci USA 1997;94:1200–1205.
[7] Moriya K, Yotsuyanagi H, Shintani Y, Fujie H, Ishibashi K, Matsuura Y, et al. Hepatitis C virus core protein induces hepatic steatosis in transgenic mice. J Gen Virol 1997;78:1527–1531.
[8] Moriya K, Todoroki T, Tsutsumi T, Fujie H, Shintani Y, Miyoshi H, et al. Increase in the concentration of carbon 18 monosaturated fatty acids in the liver with hepatitis C: analysis in transgenic mice and humans. Biophys Biochem Res Commun 2001;281:1207–1212.
[9] Lerat H, Honda M, Beard MR, Loesch K, Sun J, Yang Y, et al. Steatosis and liver cancer in transgenic mice expressing the structural and nonstructural proteins of hepatitis C virus. Gastroenterology 2002;122:352–365.